

Article

Zinc-Reduced Anticorrosive Primers—Water-Based Versus Solvent-Based

Ewa Langer ^{1,*}, Małgorzata Zubielewicz ¹, Agnieszka Królikowska ², Leszek Komorowski ²,
Katarzyna Krawczyk ³, Matthias Wanner ³, Lukas Aktas ³ and Michael Hilt ³

¹ Łukasiewicz Research Network, Institute for Engineering of Polymer Materials and Dyes, 87-100 Toruń, Poland; malgorzata.zubielewicz@impib.lukasiewicz.gov.pl

² Road and Bridge Research Institute, 03-302 Warsaw, Poland; akrolikowska@ibdim.edu.pl (A.K.); leszek.komorowski@ibdim.edu.pl (L.K.)

³ Fraunhofer Institute for Manufacturing Engineering and Automation, 70569 Stuttgart, Germany; katarzyna.krawczyk@ipa.fraunhofer.de (K.K.); matthias.wanner@ipa.fraunhofer.de (M.W.); lukas.aktas@ipa.fraunhofer.de (L.A.); michael.hilt@ipa.fraunhofer.de (M.H.)

* Correspondence: ewa.langer@impib.lukasiewicz.gov.pl

Abstract: Coating systems used for anticorrosion protection usually consist of a primer, intermediate layers, and topcoats. Zinc-rich primers, which serve as cathodic and barrier protection, are widely used for the corrosion protection of steel structures. Due to the fact that the functioning of the above-mentioned coatings is related to the conduction of galvanic current, these types of coatings are highly pigmented with zinc (up to 80 wt% in the dry coating). This may result not only in a deterioration of the performance of the coating system but also have a negative impact on the environment. Taking the above into account, solvent-based and water-based organic epoxy primers with zinc content reduced to approximately 50% have been developed. Zinc pigments of different shapes and with different surface treatments were used in the primers, as well as pigments without chemical treatment but with the addition of nanoparticles. It was found that, depending on the type of zinc pigment, both the developed solvent-based and water-based primers demonstrate good protective properties comparable to traditional zinc-rich coatings. Water-based paints tend to absorb more moisture compared to solvent-based systems, but their water uptake reversibility is limited. Moreover, the organic treatment of zinc flakes helps to improve this water uptake reversibility, improving the mechanical properties of coatings.

Keywords: solvent-based zinc; water-based zinc primers; modification of zinc pigments; corrosion protection



check for updates

Academic Editor: Binbin Zhang

Received: 22 November 2024

Revised: 3 January 2025

Accepted: 6 January 2025

Published: 8 January 2025

Citation: Langer, E.; Zubielewicz, M.; Królikowska, A.; Komorowski, L.; Krawczyk, K.; Wanner, M.; Aktas, L.; Hilt, M. Zinc-Reduced Anticorrosive Primers—Water-Based Versus Solvent-Based. *Coatings* **2025**, *15*, 64. <https://doi.org/10.3390/coatings15010064>

Copyright: © 2025 by the authors. Licensee MDPI, Basel, Switzerland. This article is an open access article distributed under the terms and conditions of the Creative Commons Attribution (CC BY) license (<https://creativecommons.org/licenses/by/4.0/>).

1. Introduction

Due to its mechanical properties, its moderate costs, and its availability in large quantities, steel is an indispensable construction material. Because of its sensitivity towards corrosion, however, corrosion protection—mostly processed by anticorrosive paint systems—is inevitable. Typically, such a paint system consists of a primer, one or several intermediate coats, and a topcoat. The function of the primer is to ensure good adhesion to the substrate and to protect it from corrosion, mainly by the surface-active compounds that are present there. For this purpose, zinc pigments are often formulated into such primers, where they act as sacrificial anodes [1,2]. This means that the substrate is protected by Zn metal or alloy that is electrochemically more active than the substrate to be protected (stage of cathodic protection) [3,4]. During the lifetime of such systems, Zn is transformed into its

corrosion products—generated through the anodic dissolution of zinc particles—which seal the pores to a point at which the system becomes electrically nonconductive (barrier stage) [5,6]. Since the performance of sacrificial coatings is based on the transfer of galvanic current, which implies metallic contact between the individual active pigments, such coatings are typically very highly pigmented [5,7–15]. High zinc content in coatings, equal to or exceeding critical pigment volume concentration (CPVC), often causes a decrease in cohesion and an increase in porosity as well as deterioration of flexibility, impact resistance, and resistance to other mechanical factors [16–18]. Therefore—and because Zn is known to be harmful to the environment—the main direction of research on new zinc-pigmented primers is to reduce its content or partially replace it with other pigments or fillers, including nanoparticles. The second direction of research in the field of zinc primers, forced by requirements regarding reducing VOC emissions into the atmosphere, is paints based on aqueous dispersions. In order to reduce the content of zinc in anticorrosive coatings, many modifications of zinc-rich primers were carried out to solve problems connected with very high pigment volume concentration (PVC). Their goal is also to improve the anticorrosive properties and extend the cathodic protection period. One possibility is an addition of nanoparticles—graphene [19–27] or carbon nanotubes (CNT) [22,26–30] as well as conductive polymers [31–35]. The use of carbon nanoparticles with a very low percolation threshold (<0.1%) makes it possible to reduce the content of zinc particles below their percolation threshold.

Jiaqing Guan and Xusheng Du [19] incorporated three-dimensional reduced graphene oxide (3DRGO) doped with N heteroatoms into the epoxy coating. 3DRGO, with a content of only 0.05 wt%, improved the corrosion resistance of coatings more than the conventional 2-dimensional reduced GO (RGO) sheets and 3D graphene (3DG) with similar 3D structures. This can be attributed to the unique three-dimensional porous structure of 3DRGO as well as N doping, which plays an important role in improving the interaction of 3DRGO with the epoxy matrix, preventing its agglomeration, improving the barrier properties of the coating, and increasing the electrical conductivity between Zn particles. An addition of graphene oxide (GO) with carboxylic, carbonyl, hydroxyl, and epoxy functional groups, which are reactive locations for covalent and non-covalent bonds with organic and inorganic compounds, to zinc primers ensured improved interaction between GO and the polymer [25,36,37]. Results showed that the incorporation of graphene oxide modified by functionalized silane coupling agent (2-(3,4-epoxycyclohexyl) ethyl triethoxysilane) improved the corrosion resistance of epoxy coatings with functionalized GO content of 0.7 wt% [25]. Graphene can be used in both solvent-based and water-based paints. Some researchers [38,39] studied the properties of water-based zinc epoxy paints with the addition of graphene in various amounts. They found that 0.6 wt% significantly extended the cathodic protection period and improved barrier protection compared to coatings containing zinc pigment alone. It was shown that the addition of graphene of 0.5 wt% was already sufficient to improve the properties of water-borne zinc epoxy primers [40,41]. The coatings had significantly better water resistance, and the corrosion rate was an order of magnitude lower compared to coatings not containing this additive. Another possibility for the partial replacement of zinc dust is to combine nanoparticles with intrinsically conductive polymers [34,42–47]. Ramezanzadeh et al. [34] carried out the studies using GO itself and with surface modification by highly crystalline and conductive polyaniline. They showed that even the addition of GO/polyaniline composites in the amount of 0.1 wt% provides both better cathodic protection and improved barrier properties of the coatings.

The improvement of the corrosion resistance of epoxy zinc coatings was also achieved by the addition of CNT with a surface modified using polypyrrole in combination with aluminum nanoparticles [43]. Nanoparticles of zinc were investigated as additives that

increase conductivity and thus improve the anticorrosive properties of zinc-rich coatings. Replacement of zinc dust (about 92 wt% Zn) with zinc nanoparticles in amounts of 5–10 wt% in zinc-rich epoxy primers may extend the cathodic protection period by increasing the electrical contact between the microparticles [48,49]. A small amount of nanoparticles in the coating also improves the second stage of protection—sealing the coating with zinc corrosion products. A small addition of a mixture consisting of nanozinc and nanoclay additives also improved both the cathodic and barrier properties of the coatings [49]. Highly efficient galvanic activity—at reduced film permeability—is often caused by better connectivity of the pigments because of the lower average distance between the particles. Interparticle distance decreases with the decreasing size of the particles, resulting in decreasing electrical percolation thresholds [50,51]. As a result of the introduction of pyrolyzed and gasified biochar nanoparticles (BCN) into a series of zinc epoxy coatings, enhanced barrier protection was achieved, especially for formulations with lower zinc content (10 vol% and 22 vol%) [52]. Gasified BCN-modified coatings with 30 vol% of zinc pigment showed more than 600 h of efficient cathodic protection. Positive results were also obtained by application in zinc-pigmented epoxy paint of nickel-20 chromium and TiO₂ nanoparticles. It was found that the added nanoparticles improved the hardness and corrosion resistance of the coating significantly [53].

The properties of zinc coatings with a lower content of Zn can be influenced by the different sizes and shapes of the zinc particles. Small zinc particles provide both very good electrical conductivity owing to the good contact between the particles and good zinc distribution in the coating [9,54]. Coatings pigmented with zinc flakes provide effective protection at a lower PVC of approx. 50% than coatings pigmented with spherical particles (PVC approx. 60%). Due to their larger specific surface area than spherical Zn particles, they ensure greater electrical contact and better surface distribution of the protective current. Kalendová [55] showed that the lamellar zinc particles exhibit the highest anticorrosive efficiency at content as low as 20 vol%. Moreover, it was found that the combination of spherical and lamellar zinc was the best in providing corrosion protection [56]. Liuyan Zhang et al. [57] obtained several series of coatings containing lamellar Zn (Al) pigments dispersed in silicone-acrylate emulsion-modified inorganic silicate vehicles. The modified coatings with a mixture of Zn and Al pigments reduced to 25 wt% provided satisfactory anticorrosive properties. Zinc flake-pigmented coatings show better cathodic protection, but at the same time, the zinc flakes dissolve faster. The addition of a small amount of anticorrosive pigments, e.g., zinc phosphate, may be helpful in solving this problem [54]. Zn, ZnAl, and ZnAlMg alloys were used to replace spherical Zn powders to develop environmentally friendly coatings with low pigment content [58]. The results showed that the coatings with the use of all flake metals instead of spherical zinc pigments were distinguished by better corrosion protection. Among them, the ZnAl coatings displayed the best anticorrosive performance. An attractive modification of zinc-pigmented coatings seemed to be an addition of zinc practices in the form of fibers. Chunping Qi et al. [59] investigated the effect of adding 0.5 wt% zinc fibers on the anticorrosive properties of coatings with 85, 75, and 65 wt% of zinc dust, but they did not find significant improvement in their anticorrosion behavior. Chemical modification of zinc particles improves the anticorrosive properties of zinc-pigmented coatings by reducing the electrochemical activity of Zn and thus slowing down their dissolution in corrosive environments. Modification with phosphoric acid 2-ethylhexyl ester and calcium ions resulted in the formation of a 190 nm alkyl-phosphate-calcium complex layer on the surface of the particles [7]. Improvement of the anticorrosive properties of coatings was achieved not only by reducing the reactivity of zinc but also by increasing the affinity between the layer formed on the zinc particle and the polymer matrix. Zinc particles modified using

aqueous organosilane (OS) solutions showed higher resistance to dissolution than non-treated zinc particles due to the formation on the surface of a zinc-OS layer approximately 10 nm thick [60]. The improvement of corrosion resistance was accomplished both by the formation of an OS layer on the zinc particles and the subsequent reaction between the functional groups of OS and the functional groups of the binder or curing agents. The highest corrosion resistance showed the coating containing zinc particles treated with bis-trimethoxysilylpropyl amine (BTSPA).

In the case of water-based zinc primers, chemical modification of Zn particles is also used to avoid hydrogen evolution due to the high reactivity of zinc with water [61]. Gassing of the paint causes defects in the coating surface as well as insufficient dispersion of zinc particles in the vehicle. In our research, we focused both on solvent-based and water-based organic epoxy primers with significantly reduced amounts of zinc pigments added in various forms and, alternatively, with nanoparticles.

2. Materials and Methods

2.1. Materials

Zinc pigments of various shapes (dust, flakes), with and without chemical treatment with silanes (wet and dry methods) and with the addition of 0.6 wt% of graphene or CNT, were used in the study. The characteristics of zinc pigments are given in Table 1, and graphene and CNT are in Table 2.

Table 1. Characteristics of zinc pigments.

Type of Pigment	Properties				
	Average Particle Size, μm	Sieve Residue at %	Density, g/cm^3	Special Surface Area, m^2/g	Content, Mass Fraction, %
Zinc (spherical)	3.6	45 μm 0.001	7.1	—	Total zinc $\geq 99.0\%$ Metallic zinc $\geq 96.5\%$ Lead $\leq 0.003\%$ Cadmium $\leq 0.0005\%$ Iron $\leq 0.002\%$ Others Traces
Zinc (flakes)	13.7	>71 μm 0.1	0.8 (bulk density)	1.2	Metal purity 99.99%

Table 2. Characteristic of graphene and CNT.

Type of Pigment	Properties			
	Average Particle Size	Density, g/cm^3	Special Surface Area, m^2/g	Content, Mass Fraction, %
Graphene	6.22 μm (D50)	<0.1 (tap density)	253.22	Carbon >93.0 Oxygen <3.0 Sulfur <0.2
CNT	20 nm	0.03–0.05	150–250	Metal oxides content: <3

The pigment treatment was carried out according to the patent [62] using isopropanol (wet method) and without isopropanol (dry method) as precipitate agents in the presence of silane. Two types of silanes were used for chemical treatment: 3-methacryloxypropyltrimethoxysilane in the dry method and 3-glycidylxypropyltrimethoxysilane in the wet method.

Solvent-based samples were prepared by dispersing Zn pigments in the two-component epoxy resin solution in xylene with an addition of butanol, additives, and

molecular sieves. The following additives were added to the model paints: an organic thixotropy agent based on a special diamide wax as a rheology modifier, micronized, highly porous, crystalline aluminosilicate with pore openings of approximately 3 Å as a molecular sieve, a solution of an alkylammonium salt of a polycarboxylic acid as a controlled flocculating wetting and dispersing additive, and a polymeric non-ionic dispersing and wetting agent—highly effective deaerator concentrate based on polyether siloxane technology.

In the case of water-based samples, Zn pigments were dispersed in anhydrous epoxy resin with additives and molecular sieves. Methoxypropanol was used as a coalescing agent. The same additives were used in the solvent base composition, and additionally, a solution of an alkylammonium salt of a polycarboxylic acid as a controlled flocculating wetting and dispersing additive and polyether siloxane copolymer as a flow promotor with deaerating properties. In both formulations, microtalc was used as an extender (the same amount was used for each formulation).

Resins and additives were premixed using a 40 mm dissolver disk at 2000 rpm for 5 min. Next, zinc pigments and extenders were added and mixed at 2000 rpm until reaching 55 °C to activate the rheology modifier and then mixed for another 10 min.

The basic properties of solvent EP resin and aqueous dispersion are given in Table 3.

Table 3. Basic properties of solvent resin and aqueous dispersion.

Property	Solvent EP Resin	Aqueous Dispersion
Dynamic viscosity, mPa·s	20,000–30,000 (25 °C)	1000–5000 (23 °C)
Epoxy equivalent, g/mol	194–208	650–780
Density, g/cm ³	1.15 (25 °C)	1.08 (20 °C)

The amount of zinc pigments in each paint was about 35 wt%, i.e., less than half of that commonly used in zinc-rich paints. For comparison, the samples of paint with 60 wt% of Zn dust were also prepared. The composition of the paint samples is presented in Table 4.

Table 4. Composition and symbols of test samples.

Symbol	Vehicle	Pigment/wt% in Paint
R0/1	Solvent-based epoxy	Zn dust/35
R0/2		Zn dust/60
R2/1		Zn flakes/35
R2/2		Zn flakes/23 + Zn dust/12
R2/3		Zn flakes/23 + Zn dust/12 + Zn phosphate/5
R3		Zn dust with wet treatment/35
R6		Zn dust/35 + graphene/0.6
R7		Zn dust/35 + CNT/0.6
F1/a	Water-based epoxy	Zn dust/60
F1/b		Zn dust/35
F1/c		Zn dust/18 + Zn flakes/7
F1/d		Zn dust/18 + Zn flakes/7 + Zn phosphate/5
F1/e		Zn dust with wet treatment/18 + Zn flakes/7
F1/f		Zn dust/18 + Zn flakes with dry treatment/7
F1/g		Zn dust/18 + Zn flakes with wet treatment/7
F1/h		Zn dust/35 + graphene/0.6
EP1	Solvent-based epoxy	Commercial zinc-rich primers for comparison
EP2		
F0	Water-based epoxy	

The protective properties of obtained coatings were tested in comparison with commercial epoxy zinc-rich primers, both solvent-based and water-based. The first solvent-based paints (marked as EP1) and water-based paints (marked as F0) are typical zinc-rich primers. The second solvent-based (marked as EP2) is an innovative primer with a high content of activated zinc, containing small hollow glass spheres with a diameter of $\sim 40\ \mu\text{m}$ and a special auxiliary agent—an activator designed to activate zinc.

The paint compositions and commercial paints were applied by the airless spray method on S235JR steel panels prepared by abrasive blasting up to Sa 2½ according to EN ISO 8501-1 [63]. The thickness of the test coatings was about $60\ \mu\text{m}$.

2.2. Methods

The protective properties of coatings with reduced content of zinc pigments and standard zinc-rich primers were studied by the following methods:

- salt spray test (SST)—salt chamber type BS1, Braive Instruments, Liège, Belgium; evaluation after 500 h, 1000 h, and 1500 h of exposure,
- scanning Kelvin probe (SKP) detection of artificially inflicted samples,
- thermocyclic electrolytic loading (TEL),
- detection of water uptake reversibility (WUR).

Investigations of the coatings' behavior under corrosive conditions were carried out by salt spray test (SST) in a salt chamber (type BS1, Braive) acc. to EN ISO 9227 [64]. The coatings were evaluated after 500, 1000, and 1500 h of SST in terms of corrosion visible on the coating. The extent of damages was assessed according to a conventional scale (from 0—no damage to 5—the most damage), taking into account indicators given in [65]. Before and after SST, mechanical properties were tested: adhesion by X-cut method (universal method for different thicknesses, often used in practice) acc. to [66] and impact resistance (measured in cm of weight drop from a height of 1 m) acc. to [67].

A scanning Kelvin probe (SKP) was used for the detection of artificially inflicted samples after corrosive impacts. The instrument allows the determination of corrosion potential differences through high-resolution, contactless measurements, even in the presence of insulating organic coatings. The best samples of zinc primers applied to Sa 2.5 steel substrates ($50\ \text{mm} \times 50\ \text{mm}$), which were exposed to salt spray testing, were placed on the sample table of either a PAR SKP100e system, controlled by a PAR SCV 100 unit, or a KP Technology SKP5050 system (Anfatec Instruments AG, Oelsnitz/Vogtl., Germany).

After alignment, the samples were scanned around a central artificial defect that exposed the substrate, created by a 1 mm drill prior to salt spray testing. This area, measuring $1\ \text{cm}^2$, was scanned using either a 0.8 mm tungsten probe or a 1 mm gold probe in the x/y direction with a resolution of 50×50 . The probe potential was calibrated relatively to a Cu/CuSO₄ electrode. All potentials are given vs. SCE.

Thermocyclic electrolytic loading (TEL) was conducted to accelerate the corrosive effects of an electrolyte solution and induce internal stress buildup, simulating the natural temperature cycling that occurs under outdoor weathering conditions. The experimental setup for this method, which enables short-term evaluation of the anticorrosive properties of coating systems, is shown in Figure 1. For this approach, a PVC cylindrical tube ($\varnothing 25\ \text{mm}$, height: 20 mm) adhered to the surface of each test panel using silicone rubber adhesive (Srintec 600, Carl Roth GmbH, Karlsruhe, Germany).

During the tests, thermocycles ranging from $10\ ^\circ\text{C}$ to $40\ ^\circ\text{C}$ in sinusoidal intervals of 1 h were applied. The temperature of the cooling plate was set to $-10\ ^\circ\text{C}$, while irradiation was provided by six evenly arranged IR emitters (G40, SPRUNGMANN Infrarottechnik GmbH, Herford, Germany). These emitters were controlled by a SIN2-PID device (ELEKTRONIKA JDROWA, Kraków, Poland), with the temperature sensor firmly attached to the surface of

one test sample. The electrolyte cells were filled with 7 mL of electrolyte solution (3% NaCl unless stated otherwise). Electrochemical impedance spectroscopy (EIS) measurements were carried out using an ATLAS 0441 High Impedance Analyzer (ATLAS-SOLLICH, Rebiechowo, Poland) in a two-electrode setup. The working electrode was the test panel substrate, while a Pt wire (\varnothing 0.5 mm) immersed in the electrolyte solution served as the counter electrode. Measurements were performed with a modulation amplitude of 25 mV across a frequency range from 100 kHz to 0.1 Hz.

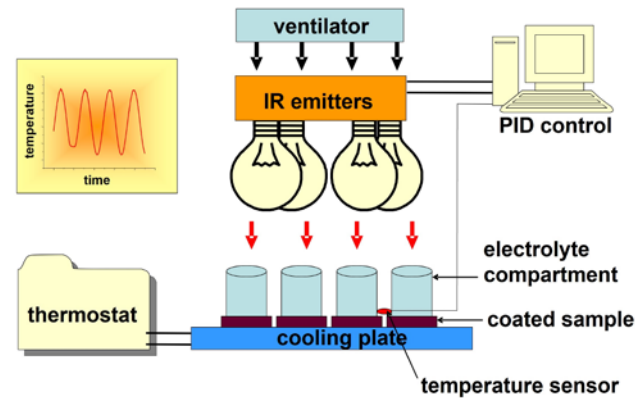


Figure 1. Experimental setup for the induction of thermocyclic electrolytic loading (TEL).

The water uptake of a coating leads to an increase in coating capacitance C_c , which is proportional to the dielectric constant ϵ_r of the detected medium. Since the ϵ_r of a typical coating ranges between 2 and 8, while ϵ_r of water (H_2O) is approximately 80, water absorption by the coating results in a noticeable increase in C_c . Therefore, C_c can be used as an indicator of water uptake. By continuously monitoring the high-frequency capacitance C_{HF} during rapid hydrothermal cycling (sinusoidal temperature variations between 15 °C and 40 °C in 30 min intervals, using 0.025 M KNO_3 as the electrolyte), performed with a Gamry Reference 600 (Gamry Instruments, Haar, Germany) in a two-electrode setup, C_{HF} vs. time diagrams can reveal changes in the dielectric properties of the primer systems induced by this cycling.

Based on EIS data, C_{HF} is calculated as follows:

$$C_{HF} = (2\pi f |Z|_{HF} \sin|\phi|_{HF})^{-1} \quad (1)$$

where HF denotes the high-frequency data from the impedance spectrum (in this case, $HF = 100$ kHz), $|Z|$ represents the impedance modulus, and ϕ the corresponding phase shift. The experimental setup is shown in Figure 2.

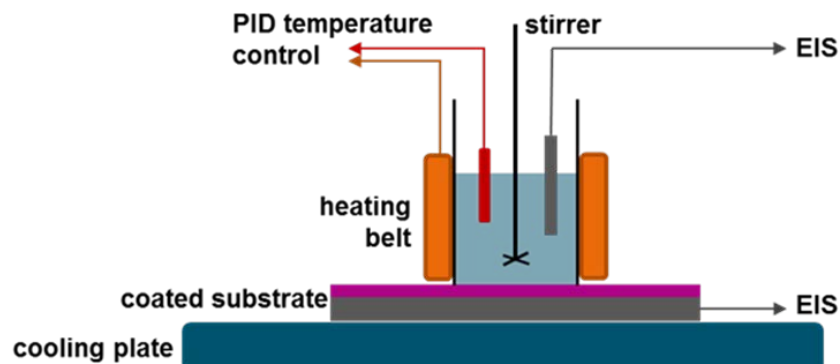


Figure 2. Experimental setup for the detection of the water uptake reversibility (WUR).

3. Results and Discussion

3.1. Visual Assessment During SST

Effective protection against corrosion is provided by coatings containing 60 wt% of Zn dust dispersed in both solvent-based and water-based resins (samples R0/2 and F1/a) (Figure 3), but some of the compositions with reduced zinc pigment content also have very good corrosion resistance.

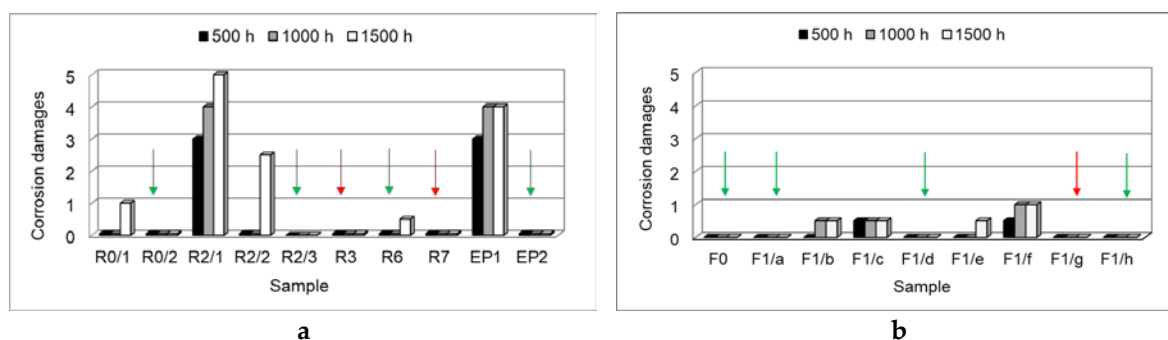


Figure 3. Comparison of anticorrosive properties of solvent-borne (a) and water-borne (b) coatings during SST. Keys: green arrows—results for both solvent-based and water-based samples; red arrows—results only for solvent-based or water-based samples.

Excellent anticorrosive properties in the corrosion environment are demonstrated by Zn pigments with wet surface treatment dispersed both in solvent-borne (sample R3) and water-borne (samples F1/c and F1/d) vehicles (Figure 3). The wet process has proven to be a more effective method of improving the corrosion resistance of coatings than the dry method (sample F1/f). Very good results were also achieved in the case of coatings containing nanoparticles of graphene (in both vehicles—samples R6 and F1/h) and CNT (in the solvent-based one—sample R7).

All of these coatings mentioned above are as effective as the epoxy-modified zinc-rich primer (EP2) and water-based F0 and exceed the properties of the other standard solvent-based primer EP1.

Similar results were achieved for formulations containing a mixture of unmodified zinc dust and unmodified zinc flakes (solvent-based R2/2, water-based F1/c). Coatings showed slightly poorer anticorrosive properties, which can be improved by the incorporation of a small amount of zinc phosphate as an anticorrosive pigment into the formulations (samples R2/3 and F1/d).

Before SST, all coatings with reduced zinc pigment content were characterized by very good mechanical properties—their adhesion measured by the X-cut method was 0, and impact resistance was 100, in contrast to the commercial EP1 coating, which had an adhesion of 3 and impact resistance of 80. During exposure to a corrosion environment, poorer adhesion showed coatings where corrosion was observed. Adhesion of the sample R2/1 decreased to 3, R2/2 to 2, and F1/f to 1.

3.2. Electrochemical Measurement

3.2.1. Thermocyclic Electrolytic Loading (TEL)

Using the device and method described in Section 2.2, the trial formulations were subjected to an accelerated simulation of seawater exposure. Previous studies have shown that the corrosion potential (E_{cor}) measured during such exposure provided data that correlated with long-term salt spray test results. From these data, a parameter, t_{bp} , could be derived, representing the exposure time required for E_{cor} (or open-circuit potential,

OCP) of the respective Zn primer test panels to reach the transition phase. The protection mechanism of zinc primer coatings can be described in three phases:

1. Phase of Cathodic Protection (PCP): During this phase, the open-circuit potential (OCP) is approximately -1.05 V to -0.86 V vs. SCE. The zinc pigments are in electrical contact with the substrate, providing cathodic protection against corrosion. This continues until the corrosion potential of the substrate ($OCP(Fe) = -0.86$ V vs. SCE) is reached.
2. Transition Phase (TP): In this phase, the OCP ranges from -0.86 V to -0.70 V vs. SCE. Zinc is progressively oxidized and no longer provides complete corrosion protection for the steel substrate.
3. Barrier Phase (BP): When the OCP exceeds -0.70 V vs. SCE, zinc no longer offers significant cathodic protection. However, the formation of bulky zinc corrosion products fills pores, which may close diffusion paths.

The thermocyclic electrolytic loading (TEL) imposes additional stress on the primers. Continuous temperature fluctuations lead to repeated contraction and expansion of the sample, causing additional stresses at the interfaces between pigment, binder, and substrate. This increases the likelihood of bond breakage within the polymer binder chains. In this short-term test, Zn-primer test panels were examined to determine the extent to which performance in the salt spray test correlates with the TEL results. The results are shown in Figure 4. Their potential values shown were measured at room temperature (approximately 20 – 25 °C) after each cycling step. The PCP phase shown in Figure 4 refers to the cathodic corrosion protection phase (PCP), which examines the potential behavior of the coating system. This phase highlights the protective effect of the coating in anodic environments, particularly in inhibiting corrosion through active layer components.

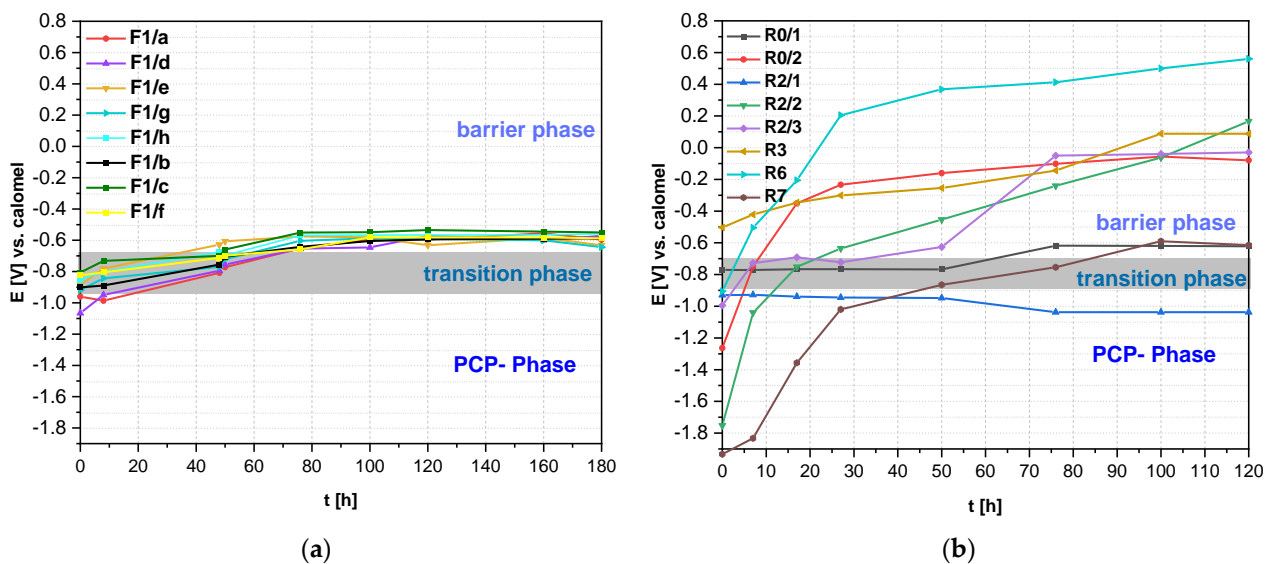


Figure 4. Comparison of E_{OC} vs. t plot of the solvent-borne (a) and water-borne (b) Zn primer systems studied during TEL exposure.

The following insights can be derived from the data displayed in Figure 4: Sample R0/1 (35% zinc dust) shows no cathodic protection, as expected. In contrast, the aqueous primer formulation F1/b reaches a potential of -0.7 V during the first 80 h of TEL but does not exceed this value. Sample R0/2 (60% zinc dust) exceeds the threshold of -0.7 V within the first 20 h of TEL but still shows no cathodic protection, while F1/a provides acceptable cathodic protection for 50 h of TEL. After an initial phase, the open circuit potential (OCP) of sample R2/1 (35% zinc flakes) drops to an active potential and exceeds -0.7 V after about

150 h. R2/2, a mixture of zinc flakes and standard zinc dust, shows much higher initial potentials and becomes “active” later but reaches the barrier phase earlier in comparison to R2/1—smaller pigments accelerate this process. In contrast, F1/c (zinc dust and zinc flakes) exceeds -0.7 V before 20 h of TEL. The formulation R2/3 (zinc dust, zinc flakes, and zinc phosphate) reaches OCP values well below -0.86 V, indicating active corrosion protection, and remains active for at least 150 h of TEL. The corresponding variant in the aqueous primer, F1/d, shows OCP values well below -0.86 V, remains active, and meets the transition phase after 60 h of TEL, indicating active corrosion protection. Sample R3 (35% surface-treated zinc pigment), however, shows no phase of cathodic protection, corresponding to a more “passive” state observed in the polarization experiment; here, OCP enters the barrier phase after 18 h. In contrast, F1/g maintains its OCP constant. R6 (35% zinc dust, 0.6% graphene) behaves similarly to F1/h but shows a brief period of cathodic protection (11 h). R7 (35% zinc dust, 0.6% CNT) briefly drops below -0.7 V but never shows signs of cathodic protection.

3.2.2. Detection of Water Uptake Reversibility (WUR)

The anticorrosion properties of a coating significantly decrease if the exchange of adsorbed water is slowed down or inhibited. Therefore, a loss of WUR can be seen as an early and sensitive indicator of imminent degradation of a coating’s anticorrosion properties. In the case of comparing water-based with VOC-based systems, the WUR is a relevant parameter that describes the resistance of a coating under the influence of cyclic damp stress.

In the case of long-lasting wet/dry cycles, it is important that coatings can completely release absorbed water; otherwise, more and more water will accumulate over time. In each case, the zinc primer samples were cycled as described. $\Delta C3$ and ΔA may be taken as a measure for the loss of WUR. Here, $\Delta C3$ represents the difference in water uptake detected at low temperatures and caused by the effect of eight temperature cycles (cf. Figure 5). In contrast, ΔA represents the difference between the capacitance amplitude obtained for the first and for the last thermocycle. Thus, it documents the thermocyclically caused loss of resistance against thermally induced water uptake.

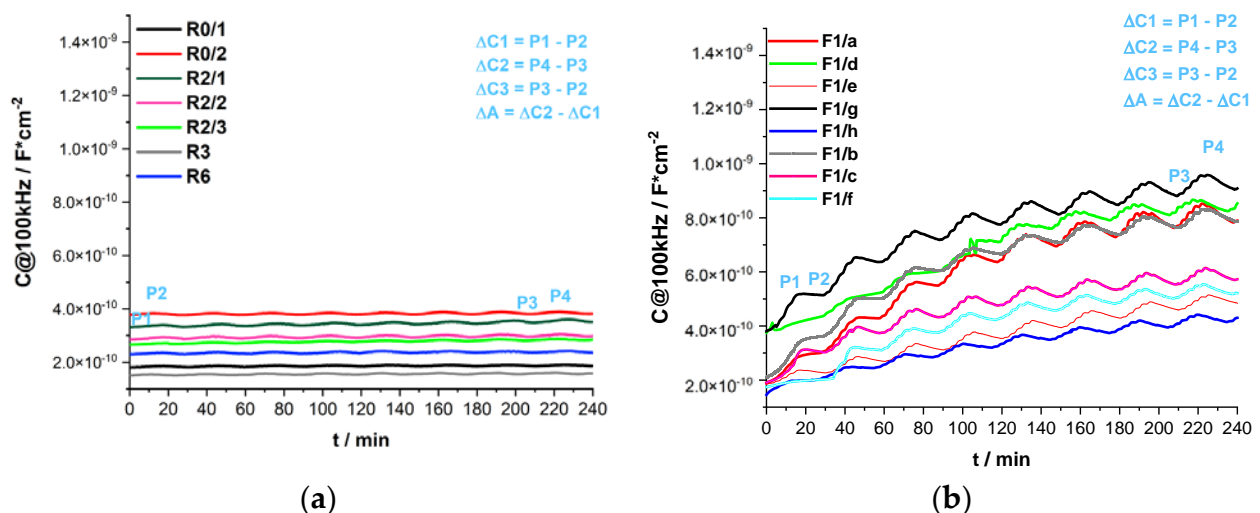


Figure 5. HF capacitance data were obtained from the solvent-borne (a) and water-borne (b) Zn primer systems.

In order to give a systematic interpretation of this data, the characteristics of these studies are listed and compared in different contexts below. The initial capacitances allow

correlations regarding the conductivities of the systems. Based on this, the following conclusions become apparent: In the analysis of water reversibility between water-based and solvent-based systems, it becomes apparent that water-based systems generally exhibit higher overall water uptake but lower water reversibility compared to solvent-based variants. Water-based primers tend to absorb more moisture, but their ability to release this moisture is limited, leading to reduced water uptake reversibility. Due to the lower polarity of organic solvents, the affinity of the coating for water is relatively low. As a result, the coating absorbs less water. The absorbed water is also efficiently released again because the solvent is not hygroscopic, and the film is less porous. Since water is a highly polar solvent, water-based coatings have a greater affinity for absorbing moisture from the environment. This leads to higher water absorption compared to solvent-based systems. At the same time, such systems tend to release water less efficiently due to the possible interactions between water and binders, as they are more hygroscopic. This can lead to some residual moisture in the film.

An interesting aspect is the behavior of the zinc particles in both systems. Samples with 60% zinc dust in spherical particle form (R0/2, F1/a) show relatively low water uptake reversibility (WUR) in the solvent-based primer when considering ΔA , in contrast to what the water-based primer shows. Figure 6 illustrates the differences in ΔA and $\Delta C3$ values obtained from both the solvent-borne and water-borne systems. In solvent-based systems, zinc supports the protective effect by drying faster, thus keeping moisture away. In water-based systems, however, water absorption can be enhanced by the hydrophilic zinc pigment, which further reduces the efficiency of water release. This suggests that the large amount of zinc in both systems forms a barrier through oxidation products such as zinc oxide and/or pore blockage that hinders the ingress and release of water. The difference in how well this works lies in the polarity of the solvents used.

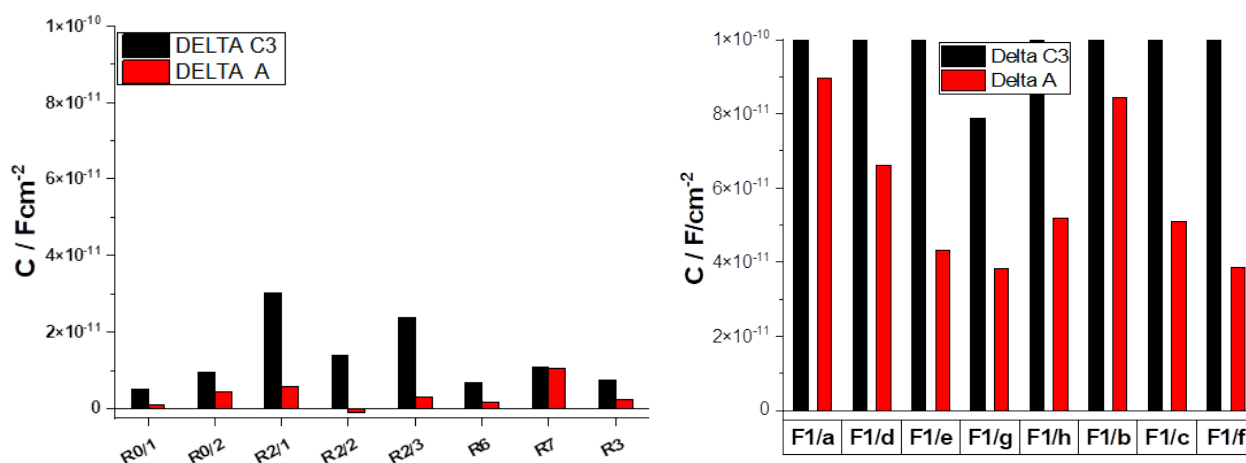


Figure 6. Differences in ΔA and $\Delta C3$ were obtained from the samples in solvent-borne (left) and water-borne (right) Zn primer systems and in the water primer.

The role of pigments, particularly zinc dust and zinc flakes, is also evident. In samples where untreated zinc particles were used, low water reversibility was observed, especially when the proportion of hygroscopic pigments like zinc phosphate was higher (R2/3, F1/d). A higher $\Delta C3$ value indicates that the coating retains an above-average amount of water. A key factor in improving water reversibility is the organic treatment of zinc flakes (R3_F1/g). Samples containing zinc flakes with wet organic treatment show improved water reversibility in both systems. The organic treatment prevents water accumulation while simultaneously improving the mechanical properties of the coatings. Notably, the use of graphene in combination with zinc particles (R6_F1/h) is particularly emphasized. In

samples containing 35% zinc dust and graphene, a significant reduction in water absorption was observed. Graphene acts here as a reinforcing agent, significantly reducing the WUR, which is attributed to an improved barrier effect.

Finally, untreated zinc flakes in both systems show significantly worse water reversibility compared to treated particles, which once again underscores the importance of particle treatment for improving water resistance and reversibility (R2/2_F1/c). Well, these two systems show (very) low DELTA A values but relatively large DELTA C3 values, so one should at least acknowledge that no significant increase in amplitude is induced in these systems; at R2/2, the amplitude of water absorption even decreases.

3.2.3. Recording of Kelvin Scans: Results

SKP detections were performed after several periods of salt spray test (SST) exposure. These detections are aimed at the determination of delamination events. Moreover, the exploration of a possible anticorrosive (cathodic) long-range effect is another goal of these detection series. In each case, the center of the scanned area (10 mm × 10 mm) was adjusted to the circular hole (ø 1.5 mm) drilled in the primer before SST exposure.

The first scan series is shown in Figure 7 and represents the SKP results of R0/2 (top) and F1/a (bottom), which were used as a model for a standard zinc-rich primer (ZRP, 60% spherical standard zinc pigment). R0/2, a typical zinc-rich primer, appears to protect the steel substrate well due to its high content of spherical zinc pigment. In the water-based primer variant F1/a, a large amount of zinc (60 wt%) provides sufficient cathodic protection to keep the entire defect area protected without any delamination occurring within the defect.

Next, we compared the systems (R3 and F1/g) with (R0/1 and F1/a), as they contain the same zinc pigmentation. However, the zinc pigments in R3 and F1/g are partially surface-treated. The R0/1 and F1/b samples contain only 35 wt% zinc pigment and provide better cathodic protection in the aqueous medium than in the solvent-based primer. In both cases, the area around the defect does not seem completely free from corrosion effects. However, as soon as the 35 wt% zinc dust is treated with an organic coating, an immediate positive effect is observed in both media. Since this is accompanied by a homogeneous cathodic zone in the defect, it can be assumed that the optimized F1g/R3 formulation induces very good cathodic protection.

The presence of an organic treatment on the zinc pigments significantly reduces the extent of the cathodic effect. Nevertheless, this treatment seems to reduce the penetration of the electrolyte at the substrate-coating interface and slows down the consumption of the zinc pigment in both the aqueous and solvent-based samples. The organic treatment also improves the adhesion of the binder matrix to the pigment and, thus, to the substrate. Therefore, the use of organically treated zinc pigments may be advantageous on a less optimally prepared substrate.

For samples with reduced zinc content and graphite addition (represented by R6 and F1/h), the solvent-based system R6 shows a complete loss of protection around the defect, although the area further from the defect appears relatively homogeneous. It is assumed that the presence of graphene improves the adhesion of the primer and significantly hinders electrolyte diffusion at the interface through the defect. In comparison, the aqueous system F1/h with graphite addition and reduced zinc content provides sufficient cathodic protection to keep the entire defect cathodically protected, with the defect itself functioning as the cathode. The addition of graphite with reduced zinc content significantly improves protection in the aqueous system, while the solvent-based system experiences a complete loss of protection around the defect.

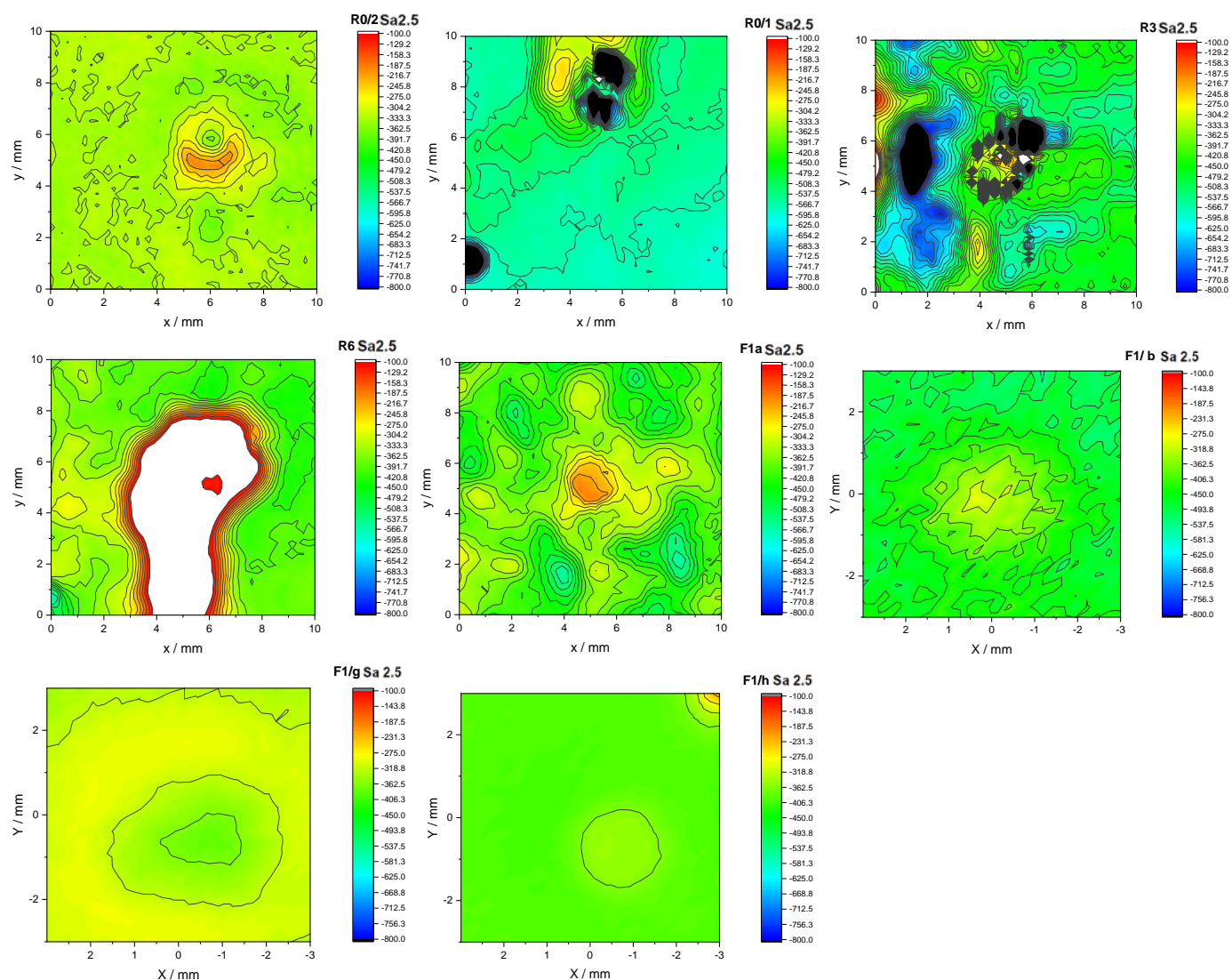


Figure 7. SKP scans obtained from Zn primers R0/2, R0/1, R3 (top), R6, F1/a, F1/b (second row), and F1/g, F1/h (bottom) obtained after 1000 h of salt spray test; the perforation inflicted by the drill (\varnothing 1.5 mm) is located approximately centrally in the scan area.

4. Conclusions

It is possible to obtain a stable water-based paint with good physical, mechanical, and anticorrosive properties using both modified and unmodified zinc pigments. The addition of zinc phosphate (5% by weight) improves the anticorrosive properties. The wet surface treatment of zinc pigments with silanes has a positive effect on improving the anticorrosive properties. Samples containing a higher content of zinc (e.g., 60 wt% zinc dust in R0/2 and F1/a) show better overall protection due to the strong barrier properties formed by zinc particles. However, the performance can be significantly enhanced with the addition of fillers and organic treatments (e.g., R2/3, F1/d). Organic treatments of zinc pigments (as in R3 and F1/g) significantly improve the cathodic protection and water resistance of coatings, as they reduce electrolyte penetration and slow zinc pigment consumption. Untreated zinc particles, particularly in higher proportions of hygroscopic pigments, lead to reduced water uptake reversibility and protection. Water-based primers tend to absorb more moisture compared to solvent-based systems, but their water uptake reversibility is limited. Organic treatment of zinc flakes helps to improve this water uptake reversibility,

preventing moisture accumulation around the pigments and improving the mechanical properties of coatings.

The addition of graphene (as in R6 and F1/h) to zinc-rich formulations reduces DELTA A, i.e., the thermocycling does not induce a large expansion of the thermally induced water uptake amplitude in these two samples and enhances the barrier effect, leading to a reduction in corrosion. While solvent-based systems with graphene show complete protection loss around defects, aqueous systems perform significantly better due to sufficient cathodic throw.

Formulations with 60 wt% zinc content (such as R0/2 and F1/a) provide sufficient cathodic throw to protect defect areas, but the overall performance can be improved by reducing zinc content and optimizing with additional particulate components such as graphite and treated pigments (e.g., in R2/3, F1/h).

Author Contributions: Conceptualization, M.Z., A.K., K.K., M.W. and M.H.; methodology, M.Z., A.K., K.K. and M.W.; investigation, M.Z., E.L., A.K., L.K., M.W., K.K. and L.A.; data curation, writing—original draft preparation, M.Z., E.L., L.K., K.K. and M.W.; supervision, M.H. All authors have read and agreed to the published version of the manuscript.

Funding: The research was carried out under the two projects: CORNET/22/1/2016, “New generation of zinc primers with improved anticorrosion, application, and ecological properties (ZINCPOWER)”, and CORNET/30/5/2020, “Water-based, environmentally friendly zinc-rich primer systems (EcoWaterZinc)”, funded by the National Centre for Research and Development (NCBiR) in Poland and the AiF within the program for the funding of industrial research (IGF) in Germany based on a decision of the German Bundestag.

Institutional Review Board Statement: Not applicable.

Informed Consent Statement: Not applicable.

Data Availability Statement: Data are contained within the article.

Conflicts of Interest: The authors declare no conflicts of interest.

References

1. Undrum, H. Silicate and Epoxy Zinc Primers: A Review. *J. Prot. Coat. Linings* **2006**, *23*, 52–57.
2. Knudsen, O.O.; Steinsmo, U.; Bjodal, M. Zinc-rich primers—Test performance and electrochemical properties. *Prog. Org. Coat.* **2005**, *54*, 224–229. [[CrossRef](#)]
3. Li, H.Y.; Duan, J.Y.; Wei, D.D. Comparison on corrosion behaviour of arc sprayed and zinc-rich coatings. *Surf. Coat. Technol.* **2013**, *235*, 259–266. [[CrossRef](#)]
4. Ramezanzadeh, B.; Arman, S.Y.; Mehdipour, M. Anticorrosion properties of an epoxy zinc-rich composite coating reinforced with zinc, aluminum, and iron oxide pigments. *J. Coat. Technol. Res.* **2014**, *11*, 727–737. [[CrossRef](#)]
5. Shreepathi, S.; Bajaj, P.; Mallik, B.P. Electrochemical impedance spectroscopy investigations of epoxy zinc rich coatings: Role of Zn content on corrosion protection mechanism. *Electrochim. Acta* **2010**, *55*, 5129–5134. [[CrossRef](#)]
6. Morcillo, M.; Barajas, R.; Felius, S.; Bastidas, J.M. A SEM study on the galvanic protection of zinc-rich paints. *J. Mater. Sci. Technol.* **1990**, *25*, 2441–2446. [[CrossRef](#)]
7. Park, J.H.; Yun, T.H.; Kim, K.Y.; Song, Y.K.; Park, J.M. The improvement of anticorrosion properties of zinc-rich organic coating by incorporating surface modified zinc particle. *Prog. Org. Coat.* **2012**, *74*, 25–35. [[CrossRef](#)]
8. Hammouda, N.; Chadli, H.; Guillemot, G.; Belmokre, K. The corrosion protection behaviour of zinc-rich epoxy paint in 3% NaCl solution. *Adv. Chem. Eng. Sci.* **2011**, *1*, 51–60. [[CrossRef](#)]
9. Vilche, J.R.; Bucharsky, E.C.; Giudice, C.A. Application of EIS and SEM to evaluate the influence of pigment shape and content in ZRP formulations on the corrosion prevention of naval steel. *Corros. Sci.* **2002**, *44*, 1287–1309. [[CrossRef](#)]
10. Hare, C.H. *Paint Film Degradation. Mechanisms and Control*; SSPC The Society for Protective Coatings: Pittsburgh, PA, USA, 2001.
11. Feliu, S.; Barajas, R.; Bastidas, J.; Morcillo, M. Mechanism of cathodic protection of zinc-rich paints by electrochemical impedance spectroscopy II. *J. Coatings Technol.* **1989**, *61*, 71–76.
12. Wicks, Z.W. *Organic Coatings: Science and Technology*, 2nd ed.; Wiley-Interscience: Hoboken, NJ, USA, 1999.

13. Baczoni, A.; Molnár, F. Advanced examination of zinc rich primers with thermodielectric spectroscopy. *Acta Polytech. Hung.* **2011**, *8*, 43–51.
14. Wang, Q. The Role of Zinc Particle Size and Loading in Cathodic Protection Efficiency. Master's Thesis, Virginia Commonwealth University VCU Scholars Compass, Richmond, VA, USA, 2012.
15. Saeedikhani, M.; Wijesinghe, S.L.; Blackwood, D.J. Barrier and Sacrificial Protection Mechanisms of Zinc Rich Primers. *Eng. J.* **2019**, *23*, 223–233. [[CrossRef](#)]
16. Zhang, W.; Xia, W.; Chen, Z.; Zhang, G.; Qian, S.; Lin, Z. Comparison of the Cathodic Protection of Epoxy Resin Coating/Zinc-Rich Coatings on Defective Areas under Atmospheric and Immersion Conditions: The Secondary Activation of Zinc Particles. *Coatings* **2024**, *14*, 336. [[CrossRef](#)]
17. Wang, J.; Qi, Y.; Zhao, X.; Zhang, Z. Electrochemical Investigation of Corrosion Behavior of Epoxy Modified Silicate Zinc-Rich Coatings in 3.5% NaCl Solution. *Coatings* **2020**, *10*, 444. [[CrossRef](#)]
18. Yan, M.; Gelling, V.J.; Hinderliter, B.R.; Battocchi, D.; Tallman, D.E.; Bierwagen, G.P. SVET method for characterizing anti-corrosion performance of metal-rich coatings. *Corros. Sci.* **2010**, *52*, 2636–2642. [[CrossRef](#)]
19. Guan, J.; Du, X. Improving the anti-corrosive performance of epoxy/zinc composite coatings with N-doped 3D reduced graphene oxide. *Prog. Org. Coat.* **2024**, *186*, 107959. [[CrossRef](#)]
20. Liu, J.; Wang, F.; Park, K.C. Study on corrosive electrochemical behaviors of zinc-rich and graphite-filled epoxy coatings in 3.5 wt% NaCl solution. *Mater. Corros.* **2011**, *62*, 1008–1014. [[CrossRef](#)]
21. Teng, S.; Gao, Y.; Cao, F.; Kong, D.; Zheng, X.; Ma, X.; Zhi, L. Zinc-reduced graphene oxide for enhanced corrosion protection of zinc-rich epoxy coatings. *Prog. Org. Coat.* **2018**, *123*, 185–189. [[CrossRef](#)]
22. Zhou, S.; Wu, Y.; Zhao, W.J.; Yu, J.; Jiang, F.; Wu, Y.; Ma, L. Designing reduced graphene oxide/zinc rich epoxy composite coatings for improving the anticorrosion performance of carbon steel substrate. *Mater. Des.* **2019**, *169*, 107694. [[CrossRef](#)]
23. Sari, M.G.; Shamshiri, M.; Ramezanzadeh, B. Fabricating an epoxy composite coating with enhanced corrosion resistance through impregnation of functionalized graphene oxide-co-montmorillonite Nanoplatelet. *Corros. Sci.* **2017**, *129*, 38–53. [[CrossRef](#)]
24. Hayatdavoudi, H.; Rahsepar, M. A mechanistic study of the enhanced cathodic protection performance of graphene-reinforced zinc rich nanocomposite coating for corrosion protection of carbon steel substrate. *J. Alloys Compd.* **2017**, *727*, 1148–1156. [[CrossRef](#)]
25. Zhang, C.; Dai, X.; Wang, Y.; Sun, G.; Li, P.; Qu, L.; Sui, Y.; Dou, Y. Preparation and Corrosion Resistance of ETEO Modified Graphene Oxide/Epoxy Resin Coating. *Coatings* **2019**, *9*, 46. [[CrossRef](#)]
26. Zubielewicz, M.; Langer, E.; Królikowska, A.; Komorowski, L.; Wanner, M.; Krawczyk, K.; Aktas, L.; Hilt, M. Concepts of steel protection by coatings with a reduced content of zinc pigments. *Prog. Org. Coat.* **2021**, *161*, 106471. [[CrossRef](#)]
27. Zubielewicz, M.; Langer, E.; Kuczyńska, H.; Królikowska, A.; Komorowski, L. The new generation of anticorrosive zinc primers with improved protective, utility and ecological properties. *Ochr. Koroz.* **2019**, *62*, 297–305.
28. Park, S.; Shon, M.J. Effects of multi-walled carbon nano tubes on corrosion protection of zinc rich epoxy resin coating. *J. Ind. Eng. Chem.* **2015**, *21*, 1258–1264. [[CrossRef](#)]
29. Cubides, Y.; Castaneda, H. Corrosion protection mechanisms of carbon nanotube and zinc-rich epoxy primers on carbon steel in simulated concrete pore solutions in the presence of chloride. *Corros. Sci.* **2016**, *109*, 145–161. [[CrossRef](#)]
30. Cubides, Y.; Su, S.S.; Castaneda, H. Influence of zinc content and chloride concentration on the corrosion protection performance of zinc-rich epoxy coatings containing carbon nanotubes on carbon steel in simulated concrete pore environments. *Corrosion* **2016**, *72*, 1397–1423. [[CrossRef](#)]
31. Marchebois, H.; Keddou, M.; Savall, C.; Bernard, J.; Touzain, S. Zinc-rich powder coatings characterisation in artificial sea water: EIS analysis of the galvanic action. *Electrochim. Acta* **2004**, *49*, 1719–1729. [[CrossRef](#)]
32. Feliú, S., Jr.; Bastidas, R.; José, M.; Morcillo, M. Effect of the Di-iron phosphide conductive extender on the protective mechanisms of zinc-rich coatings. *J. Coat. Technol.* **1991**, *63*, 67–72.
33. Armelin, E.; Martí, M.; Liesa, F.; Iribarren, J.I.; Alemán, C. Partial replacement of metallic zinc dust in heavy duty protective coatings by conducting polymer. *Prog. Org. Coat.* **2010**, *69*, 26–30. [[CrossRef](#)]
34. Ramezanzadeh, B.; Mohamadzadeh Moghadam, M.H.; Shohani, N.; Mahdavian, M. Effects of highly crystalline and conductive polyaniline/graphene oxide composites on the corrosion protection performance of a zinc-rich epoxy coating. *Chem. Eng. J.* **2017**, *320*, 363–375. [[CrossRef](#)]
35. Akbarinezhad, E. Synthesis of conductive polyaniline-graphite nanocomposite in supercritical CO₂ and its application in zinc-rich epoxy primer. *J. Supercrit. Fluids* **2014**, *94*, 8–16. [[CrossRef](#)]
36. Ramezanzadeh, B.; Ghasemi, E.; Mahdavian, M.; Changizi, E.; Moghadam, M.M. Characterization of covalently-grafted polyisocyanate chains onto graphene oxide for polyurethane composites with improved mechanical properties. *Chem. Eng. J.* **2015**, *281*, 869–883. [[CrossRef](#)]
37. Ahmadi, A.; Ramezanzadeh, B.; Mahdavian, M. Hybrid silane coating reinforced with silanized graphene oxide nanosheets with improved corrosion protective performance. *RSC Adv.* **2016**, *6*, 54102–54112. [[CrossRef](#)]

38. Zhou, L.; Zhang, P.; Shen, L.; Chu, L.; Wu, J.; Ding, Y.; Zhong, B.; Zhang, X.; Bao, N. Modified graphene oxide/waterborne epoxy composite coating with enhanced corrosion resistance. *Prog. Org. Coat.* **2022**, *172*, 107100. [CrossRef]
39. Huang, S.; Kong, G.; Yang, B.; Zhang, S.; Che, C. Effects of graphene on the corrosion evolution of zinc particles in waterborne epoxy zinc-containing coatings. *Prog. Org. Coat.* **2020**, *140*, 105531. [CrossRef]
40. Liu, S.; Gu, L.; Zhao, H.; Chen, J.; Yu, H. Corrosion Resistance of Graphene-Reinforced Waterborne Epoxy Coatings. *J. Mater. Sci. Technol.* **2016**, *32*, 425–431. [CrossRef]
41. Zhang, J.H.; Xie, J. Synergistic Effect between Zinc Particles and Graphene on the Anti-Corrosion Performance of Epoxy Coatings. *Int. J. Electrochem. Sci.* **2022**, *17*, 221238. [CrossRef]
42. Gergely, A.; Pászti, Z.; Bertóti, I.; Judith Mihály, J.; Eszetr Drotár, E.; Török, T. Hybrid Zinc-Rich Paint Coatings: The Impact of Incorporation of Nano-Size Inhibitor and Electrical Conducting Particles. Chapter 6. In *Intelligent Coatings for Corrosion Control*; Elsevier Inc.: Amsterdam, The Netherlands, 2014; Available online: <https://www.researchgate.net/publication/282595539> (accessed on 28 August 2024).
43. Gergely, A.; Pászti, Z.; Bertóti, I.; Török, T.; Mihály, J.; Kálmán, E. Novel zinc-rich epoxy paint coatings with hydrated alumina and carbon nanotubes supported polypyrrole for corrosion protection of low carbon steel: Part II: Corrosion prevention behavior of the hybrid paint coatings. *Mater. Corros.* **2013**, *64*, 1091–1103. [CrossRef]
44. Ionita, M.; Pruna, A. Polypyrrole/carbon nanotube composites: Molecular modeling and experimental investigation as anti-corrosive coating. *Prog. Org. Coat.* **2011**, *72*, 647–652. [CrossRef]
45. Martina, V.; De Riccardis, M.F.; Carbone, D.; Rotolo, P.; Bozzini, B.; Mele, C. Electrodeposition of polyaniline–carbon nanotubes composite films and investigation on their role in corrosion protection of austenitic stainless steel by SNIFTIR analysis. *J. Nanopart. Res.* **2011**, *13*, 6035–6047. [CrossRef]
46. Salam, M.A.; Al-Juaid, S.S.; Qusti, A.H.; Hermas, A. Electrochemical deposition of a carbon nanotube-poly(o-phenylenediamine) composite on a stainless steel surface. *Synth. Met.* **2011**, *161*, 153–157. [CrossRef]
47. Chen, Z.; Cai, Y.; Lu, Y.; Cao, Q.; Lv, P.; Zhang, Y.; Liu, W. Preparation and Performance Study of Carboxy-Functionalized Graphene Oxide Composite Polyaniline Modified Water-Based Epoxy Zinc-Rich Coatings. *Coatings* **2022**, *12*, 824. [CrossRef]
48. Schaefer, K.; Miszczyk, A. Improvement of electrochemical action of zinc-rich paints by addition of nanoparticulate zinc. *Corros Sci.* **2013**, *66*, 380–391. [CrossRef]
49. Arianpouya, N.; Shishesaz, M.; Ashrafi, A. Evaluation of synergistic effect of nanozinc/nanoclay additives on the corrosion performance of zinc-rich polyurethane nanocomposite coatings using electrochemical properties and salt spray testing. *Surf. Coat. Technol.* **2013**, *216*, 199–206. [CrossRef]
50. Patchan, M.W.; Baird, L.M.; Rhim, Y.-R.; LaBarre, E.D.; Maisano, A.J.; Deacon, R.M.; Xia, Z.; Benkoski, J.J. Liquid-filled metal microcapsules. *ACS Appl. Mater. Interfaces* **2012**, *4*, 2406–2412. [CrossRef] [PubMed]
51. Jing, X.; Zhao, W.; Lan, L. The effect of particle size on electric conducting percolation threshold in polymer/conducting particle composites. *J. Mater. Sci. Lett.* **2000**, *19*, 377–379. [CrossRef]
52. Li, Z.; Bi, H.; Weinell, C.E.; Ravenni, G.; Benedini, L.; Dam-Johansen, K. Investigation of zinc epoxy coatings modified with pyrolyzed and gasified biochar nanoparticles for corrosion protection. *Prog. Org. Coat.* **2023**, *178*, 107477. [CrossRef]
53. Jabbar, M.A.; Hassan, A.D.; Hamza, Z.A. Organic zinc-rich protective coatings with improved electrochemical properties: The role of nano-powder additions. *Cogent Eng.* **2021**, *8*, 1870793. [CrossRef]
54. Decelles, G. Corrosion protection systems based on lamellar zinc pigments. In Proceedings of the European Corrosion Congress EUROCORR 2018, Kraków, Poland, 9–13 September 2018.
55. Kalendová, A. Effects of particle sizes and shapes of zinc metal on the properties of anticorrosive coatings. *Prog. Org. Coat.* **2003**, *46*, 324–332. [CrossRef]
56. Jagtap, R.N.; Patil, P.P.; Hassan, S.Z. Effect of zinc oxide in combating corrosion in zinc-rich primer. *Prog. Org. Coat.* **2008**, *63*, 389–394. [CrossRef]
57. Zhang, L.; Ma, A.; Jiang, J.; Song, D.; Chen, J.; Yang, D. Anti-corrosion performance of waterborne Zn-rich coating with modified silicon-based vehicle and lamellar Zn (Al) pigments. *Prog. Nat. Sci. Mater. Int.* **2012**, *22*, 326–333. [CrossRef]
58. Zhang, J.; Zhu, Q.; Wang, Z.; Wang, X.; Yan, J. Flake-like ZnAl alloy powder modified waterborne epoxy coatings with enhanced corrosion resistance. *Prog. Org. Coat.* **2023**, *183*, 107780. [CrossRef]
59. Qi, C.; Weinell, C.E.; Dam-Johansen, K.; Wu, H. Assessment of Anticorrosion Performance of Zinc-Rich Epoxy Coatings Added with Zinc Fibers for Corrosion Protection of Steel. *ACS Omega* **2023**, *8*, 1912–1922. [CrossRef]
60. Yun, T.H.; Park, J.H.; Kim, J.-S.; Park, J.M. Effect of the surface modification of zinc powders with organosilanes on the corrosion resistance of a zinc pigmented organic coating. *Prog. Org. Coat.* **2014**, *77*, 1780–1788. [CrossRef]
61. Heine, F.; Bouuaert, P.; Wauters, N.; Elmore, J.; Erdem, B.; Crawford, D. Waterborne Epoxy Zinc-Rich Primers: There Are Viable Options. Available online: www.pcimag.com/articles/96850 (accessed on 4 September 2012).
62. Schlenk Metallic Pigments GmbH, Fraunhofer-Gesellschaft zur Förderung der angewandten Forschung e. V. Method for Modifying the Surface of Particles. International Patent Application WO 2013/156615 A1, 19 April 2013.

63. *EN ISO 8501-1:2007*; Preparation of Steel Substrates Before Application of Paints and Related Products—Visual Assessment of Surface Cleanliness—Part 1. Rust Grades and Preparation of Uncoated Steel substrates and Steel Substrates After Overall Removal of Previous Coatings. International Organization for Standardization: Geneva, Switzerland, 2007.
64. *EN ISO 9227:2022*; Corrosion Tests in Artificial Atmospheres—Salt Spray Test. International Organization for Standardization: Geneva, Switzerland, 2022.
65. *EN ISO 4628-1:2016*; Paints and Varnishes—Evaluation of Degradation of Coatings—Designation of Quantity and Size of Defects, and of Intensity of Uniform Changes in Appearance—Part 1: General Introduction and Designation System. International Organization for Standardization: Geneva, Switzerland, 2016.
66. *EN ISO 16276-2:2007*; Corrosion Protection of Steel Structures by Protective Paint Systems—Assessment of, and Acceptance criteria for, the Adhesion/Cohesion (Fracture Strength) of a Coating—Part 2: Cross-Cut Testing and X-Cut Testing. International Organization for Standardization: Geneva, Switzerland, 2007.
67. *EN ISO 6272-1:2011*; Paints and Varnishes—Rapid-Deformation (Impact Resistance) Tests—Part 1: Falling-Weight Test, Large-Area Indenter. International Organization for Standardization: Geneva, Switzerland, 2011.

Disclaimer/Publisher’s Note: The statements, opinions and data contained in all publications are solely those of the individual author(s) and contributor(s) and not of MDPI and/or the editor(s). MDPI and/or the editor(s) disclaim responsibility for any injury to people or property resulting from any ideas, methods, instructions or products referred to in the content.